Active Vibration Control of a Super Element Model of a Thin-walled Structure

Nader Ghareeb[1] and Rüdiger Schmidt[2]

[1]*Department of Mechanical Engineering, Australian College of Kuwait, Kuwait City, Kuwait*

[2]*Institute of General Mechanics, RWTH Aachen University of Technology, Aachen, Germany*

Keywords: Super Element, Lyapunov Stability Function Controller, Positive Position Feedback, Strain Rate Feedback.

Abstract: Reducing vibration in flexible structures has become a pivotal engineering problem and shifted the focus of many research endeavors. One technique to achieve this target is to implement an active control system. A conventional active control system is composed of a vibrating structure, a sensor to perceive the vibration, an actuator to counteract the influence of disturbances causing vibration, and finally a controller to generate the appropriate control signals. In this work, different linear controllers are used to attenuate the vibrations of a cantilevered smart beam excited by its first eigenmode. A finite element (FE) model of the smart beam is initially created and then modified by using experimental data. The FE model is then reduced to a super element (SE) model with a finite number of degrees of freedom (DOF). Controllers are applied directly to the SE and the results are presented and compared.

1 INTRODUCTION

In modern engineering, weight optimization has a priority during the design of structures. However, optimizing the weight results in lower stiffness and less internal damping, causing the structure to become excessively prone to vibration. Vibration can lead to additional noise, a decrease in stability, and even to the failure of the structure itself (Ghareeb and Radovcic, 2009). To overcome this problem, active or smart materials are implemented. The coupled electromechanical properties of smart materials, which are illustrated here in the form of piezoelectric ceramics, make these smart materials well-suited for being used as distributed sensors and actuators for controling structural response. Although the piezoelectric effect was first mentioned by Haüy in 1817 and demonstrated by Pierre and Jacques Curie in 1880, the use of piezoelectric materials as actuators and sensors for noise and vibration control has only been demonstrated extensively over the past thirty years (Piefort, 2001). Bailey (Bailey, 1984) designed an active vibration damper for a cantilever beam using a distributed parameter actuator consisting of a piezoelectric polymer. Bailey and Hubbard (Bailey and Jr., 1985) developed and implemented three different control algorithms to control the cantilevered beam vibration with piezoactuators. Further, Crawley and de Luis (Crawley and de Luis, 1987) and Crawley and Anderson (Crawley and Anderson, 1990) presented a rigorous study on the stress-strain-voltage behaviour of piezoelectric elements bonded to beams. They observed that the effective moments resulting from piezoactuators can be regarded as concentrated at both ends of the actuator while assuming a very thin bonding layer.

The practical implementation and use of the piezoelectric actuators has been investigated in studies such as (Fanson and Chen, 1986) and (Moheimani and Fleming, 2006). This work emphasizes the capabilities and applications of piezoelements as distributed vibration actuators and sensors by simultaneously controling a finite number of the infinite set of modes of the actual system. On the other hand, the majority of investigations were carried out either through experiments on the real model as in (Waghulde et al., 2010),(Block and Strganan, 1998), or by using $2D$ or $3D$ FE models of the smart structure as in (Varadan et al., 1996),(Allik and Hughes, 1970). However, in the FE work, the damping coefficients were not calculated but rather assumed, which may not reflect the exact performance of the real model.

The present work comprises the modeling and design of different active linear controllers to attenuate the vibration of a cantilevered smart beam excited by its first eigenmode. The piezoactuator is initially

modeled, and the relation between the voltage and the moments at its ends is investigated. A modified *FE* model of the smart beam based on first-order shear deformation theory (*FOSD*) is then created. The damping coefficients are calculated and added to the *FE* model prior to the reduction to a *SE* model with a finite number of *DOF*. The *FE* and *SE* models are validated by performing a modal analysis and comparing the results with the experimental data. Finally, two different control strategies are introduced and implemented on the *SE* model of the smart beam: Positive position feedback (*PPF*), and strain rate feedback (*SRF*). Results are then compared to the results of applying a Lyapunov stability function controller which was developed in (Ghareeb and Schmidt, 2012). The *FE* package SAMCEF is used for the creation of both the *FE* and *SE* models, as well as for the implementation of the controllers in the *SE* model.

2 MODELING

The first step in designing a control system is to build a full representative mathematical model of the real system including all the disturbances causing the unwanted vibration. The structural analytical model can be derived either from physical laws (Newton's motion laws, Lagrange's equations of motion, D'Alembert principle, etc), from test data using system identification methods (stochastic subspace identification, prediction error method, etc), or by using the *FE* method (Gawronski, 2004). The smart beam used in this work consists of a steel beam, a bonding layer and an actuator as seen in Figure 1.
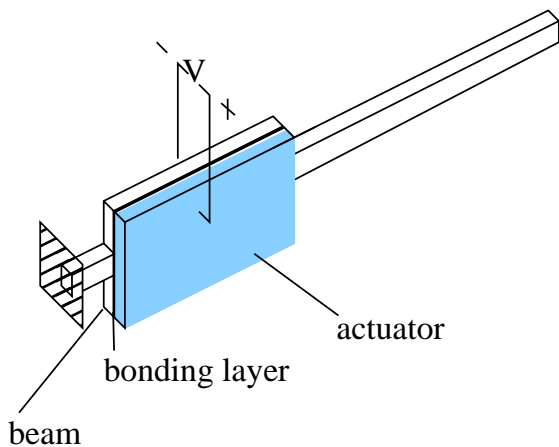

Figure 1: The smart beam.

2.1 Actuator Modeling

Using an actuator means imposing an appropriate electric potential to control the vibration in the smart structure (converse piezoelectric effect). Many *FE* packages do not offer elements with electrical *DOF*. On the other hand, the voltage applied by the actuator can be represented by two equal moments with opposite directions concentrated at its ends (Fanson and Chen, 1986). The relation between actuator moments and voltage can be investigated, so that equivalent moments are used instead as input to the controller as illustrated in Figure 2. The structure is modeled as one dimensional and the behavior of the piezoelectric material is assumed to be linear throughout this work.
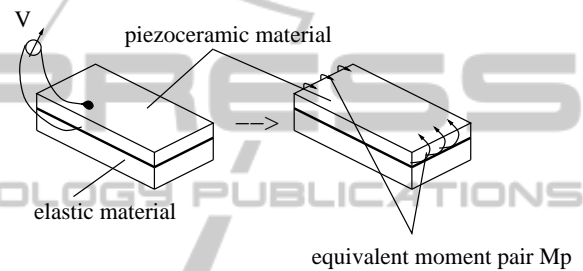

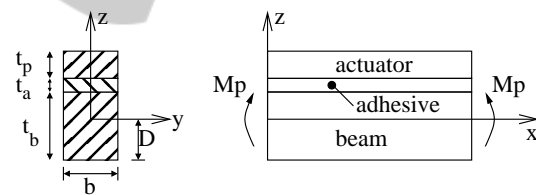Figure 2: The induced stresses from a piezoceramic actuator.

Figure 3: A schematic layout of the smart beam.

Considering the schematic layout of the middle portion of the smart beam in Figure 3, if a voltage *V* is applied accross the piezoelectric actuator while assuming one dimensional deformation, the piezoelectric strain ε_p in the piezo is

$$\varepsilon_p = \frac{d_{31}}{t_p} \cdot V \qquad (1)$$

with *V* as the voltage of the piezo-electric actuator, d_{31} the electric charge constant and t_p the thickness of the actuator.

Using Hooke's law, the longitudinal stress is defined as

$$\sigma_p = E_p \cdot \varepsilon_p = E_p \cdot \frac{d_{31}}{t_p} \cdot V \qquad (2)$$

Where E_p is the Young's modulus of elasticity of the piezoceramic actuator.

This stress generates a bending moment M_p around the neutral axis of the composite beam given by

$$M_p = \int_{(t_a+t_b-D)}^{(t_p+t_a+t_b-D)} \sigma_p \cdot b \cdot z \, \mathrm{d}z \qquad (3)$$

t_a and t_b are the thickness values of the adhesive layer and the beam, b is the width of the composite layer at beam's middle, and D the distance from beam's bottom to the neutral axis.

Considering equilibrium of moments about the neutral axis gives

$$\int_{piezo} \sigma_p \, \mathrm{d}A + \int_{adhesive} \sigma_a \, \mathrm{d}A + \int_{beam} \sigma_b \, \mathrm{d}A = 0 \qquad (4)$$

This means,

$$E_p b \int_{(t_a+t_b-D)}^{(t_p+t_a+t_b-D)} z \, \mathrm{d}z + E_a b \int_{(t_b-D)}^{(t_a+t_b-D)} z \, \mathrm{d}z +$$
$$E_b b \int_{(-D)}^{(t_b-D)} z \, \mathrm{d}z = 0 \qquad (5)$$

t_p is the thickness of the beam, E_a the Young's modulus of the adhesive and E_b the Young's modulus of the steel beam.

$$D = \frac{E_p t_p^2 + 2E_p t_p t_a + 2E_p t_p t_b + E_a t_a^2 + 2E_a t_a t_b + E_b t_b^2}{2E_p t_p + 2E_a t_a + 2E_b t_b} \qquad (6)$$

Substituting (6) and (2) in (3) determines the bending moment generated by the piezo M_p as a function of the voltage V

$$M_p = \frac{E_p E_a (t_p t_a + t_a^2) + E_p E_b (t_b^2 + t_p t_b + 2t_a t_b)}{E_p t_p + E_a t_a + E_b t_b} \cdot \frac{d \cdot b}{2} \cdot V \qquad (7)$$

Since the relation between M_p and V is now known, the actuator moments will be taken instead of the voltage as the input to the controllers that are designed and implemented in the next sections. The importance of this achievement is that only mechanical *DOF* will be included in the model.

2.2 *FE* Modeling of the Smart Beam

Many applications in structural dynamics can be successful only when they are represented by an accurate mathematical model. A way to derive this model is to use *FE* modeling. In order to find the best *FE* model that represents the smart beam, the optimal type and size of the finite elements must be selected. For this reason, a modal analysis of the real beam is indispensable. The modal analysis is experimentally performed, and results of the natural frequencies are compared with those from the *FE* model. A detailed geometry of the smart beam is shown in Figure 4, and the material properties and thickness of each part are represented in Table 1.
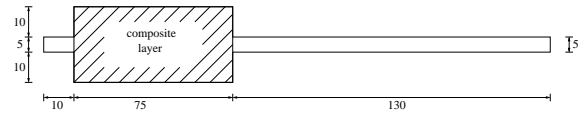
Figure 4: A detailed geometry of the smart beam [dimensions in *mm*].

Table 1: Parameters of the components of the smart beam.

	Beam	Bonding	Actuator
Material	steel	epoxy	PIC 151
Thickness [*mm*]	0.5	0.036	0.25
Density [kg/m^3]	7900	1180	7800
Young's mod. [*MPa*]	210000	3546	66667

The smart beam is created as a unique structure but modeled as a composite shell with three layers without any relative slip among their contact surfaces. Furthermore, a composite shell element with eight nodes based on the *FOSD* is used. To valiate the *FE* model, a modal analysis is performed and the first two eigenfrequencies are read and compared to those from the experiment. This is presented in Table 2. As a boundary condition, the far left edge of the smart beam is clamped.

Table 2: validation of element-type based on the modal analysis.

	FE model	Experiment
1st eigenfreq. [*Hz*]	13.81	13.26
2nd eigenfreq. [*Hz*]	42.67	41.14

2.2.1 Damping Characteristics

Damping parameters, which are of significant importance in determining the dynamic response of structures, cannot be deduced deterministically from other structural properties or even predicted by using the *FE* technique. For simplicity and convenience the damping is assumed to be viscous and frequency dependent (Alipour and Zareian, 2008). This linear approach assumes that the damping matrix is a linear combination of the mass and stiffness matrices. Although this idea was suggested for mathematical convenience only, yet it allows the damping matrix to be diagonalized simultaneously with the mass and stiffness matrices, preserving the simplicity of uncoupled real normal modes as in the undamped case (Adhikari and Woodhouse, 2001).

The relation is

$$C = \alpha M + \beta K \qquad (8)$$

where α and β are real scalars that need to be determined.

To find out α and β, many methods can be applied like the method of Chowdhury and Dasgupta, or the method of damping from normalised spectra (also known as the half-power bandwidth method). These methods and the way to find the results hereafter are explained in details in (Ghareeb, 2013). Both methods are used in this work and the results are depicted in Table 3.

Table 3: Results of α and β using both methods.

Parameter	Chowdhury	Half-power
α	0.02577	0.02955
β	9.918×10^{-6}	9.77×10^{-6}

3 THE SUPER ELEMENT TECHNIQUE

The main advantage of this technique (also called substructure technique) is the ability to perform the analysis of a complete structure by using the results of prior analysis of different regions comprising the whole structure. When a preliminary analysis of the different parts is performed, the computation time and the size of the whole system are reduced. However, all *DOF* considered useless for the final solution are condensed and the rest is retained. This means, the *DOF* of the whole system will correspond to the retained nodes plus a number of internal deformation modes, (refer to SAMCEF tutorials). To construct a *SE*, or in other words to remove the unwanted nodes and *DOF* from the substructure, many methods are available. In this work, The "Component-mode method", Also known as Craig-Bampton method, is used (Craig and Bampton, 1968).

3.1 *SE* Modeling

Before the *SE* is created, the retained nodes and the condensed nodes must be designated and the number of internal modes to be used must be specified. Once again, the number of modes must respond to atleast ninety-five percent participation of the mass. Based on the current work, ten internal modes are used. The retained nodes are usually those where boundary conditions are applied, or where stresses,

displacements, etc. are imposed or measured. On these nodes the clamp is added and the actuators and sensors are placed. All other nodes are considered as condensed nodes. Concerning the smart beam used in this work, there are five retained nodes in the *SE* model (Figure 5) listed below:

- The *SE* is clamped at node 1
- The actuator moments, which will be the inputs to the controller, are added at the nodes 2 and 3
- An additional sensor to measure the vibrations is added at node 4 (to be used in future works)
- The sensor that measures the tip displacement is located at node 5

Figure 5: The retained nodes of the *SE*.

3.2 Comparison between *FE* and *SE* Model

In Table 4, a comparison between both models was done. The number of elements, nodes, and *DOF* was reduced and this has lead to a smaller structure and thus less computation time.

Table 4: Comparison between *FE* and *SE* model.

	FE model	*SE* model
Number of nodes	8206	5
Number of elements	2575	1
DOF	49236	40

3.3 Validation of the *SE* Model

As shown in Table 5, results of modal analyses of both models did not show a big difference concerning the first four eigenfrequencies. Since the excitation is done only with the first eigenfrequency, further readings were not necessary. The *SS* representation is then created upon specifying the type and position of the inputs and outputs of the model.

Table 5: Comparison between the eigenfrequencies.

Eigenfreq. no.	*FE* model	*SE* model	% Error
1	13.811	14.249	3.07
2	42.673	43.414	1.71
3	145.49	152.54	4.62
4	150.16	154.38	2.73

4 CONTROLLER DESIGN

The performance of smart structures for active vibration control depends strongly on the control algorithm accompanied with it. In this part, the aim is to design some controllers capable of damping the vibration once the smart beam is excited by its first eigenmode. After the excitation, the beam is left to vibrate freely. Exactly at this moment, the controllers are activated. Two vibration suppression methods are used in this work: The positive position feedback control (*PPF*) and the strain rate feedback control (*SRF*).

4.1 Positive Position Feedback Control (*PPF*)

This method was firstly proposed by Goh and Caughey for the collocated sensors and actuators (Goh and Caughey, 1985). Later on, it was used by Fanson and Caughey to control large space structures (Fanson and Caughey, 1990). The basic concept of the *PPF* is to feed the structural position coordinate directly to the compensator and the product of the compensator and a scaler gain positively back to the structure.

The scalar equations governing the vibration of the structure in a single mode and the *PPF* controller are given as

$$\ddot{\xi} + 2\zeta\omega\dot{\xi} + \omega^2\xi = G\omega^2\eta \qquad (9)$$

$$\ddot{\eta} + 2\zeta_c\omega_c\dot{\eta} + \omega_c^2\eta = \omega_c^2\xi \qquad (10)$$

where ξ is the structural modal coordinate, η the compensator modal coordinate, G the feedback gain, and ζ and ζ_c are the damping ratios, and ω and ω_c the natural frequencies of structure and compensator.

Since all the parts of the smart beam are integrated in a single *SE* and the damping coefficients for the whole system are calculated and the first eigenmode of the model is excited, this means

$$\zeta_c = \zeta \qquad (11)$$

$$\omega_c = \omega \qquad (12)$$

To validate this supposition, the structure motion at the steady state for a single *DOF* system can have the form

$$\xi(t) = \alpha e^{i\omega t} \qquad (13)$$

and the compensator will then respond as

$$\eta(t) = \beta e^{i(\omega t - \phi)} \qquad (14)$$

where the phase angle ϕ and the magnitude β are

$$\phi = \tan^{-1}\left(\frac{2\zeta_c(\omega/\omega_c)}{1 - (\omega/\omega_c)^2}\right)$$

$$\beta = \frac{\alpha}{\sqrt{[1 - (\omega/\omega_c)^2]^2 + [2\zeta_c(\omega/\omega_c)]^2}}$$

Since the structure and compensator have same frequency as it was assumed before, then

$$\frac{\omega}{\omega_c} = 1$$

For this reason $\phi = \frac{\pi}{2}$, and $\beta = \frac{\alpha}{2\zeta_c}$

Substituting ϕ and β in (13) and (14), and then back-substituting in (9) gives

$$\ddot{\xi} + (2\zeta w + \frac{Gw}{2\zeta_c})\dot{\xi} + w^2\xi = 0 \qquad (15)$$

Comparing (15) to (9), it can be seen that with the assumption of equal frequencies between the structure and the compensator, there is an increase in the damping ratio, which is called active damping.

A Nyquist stability analysis of the system of scalar equations (9) and (10) results in the necessary and sufficient condition for stability

$$\text{stability if } 0 < G < 1$$

Implementing the *PPF* controller in the smart structure used in this work, has damped the tip displacement as can be seen in Figure 6.
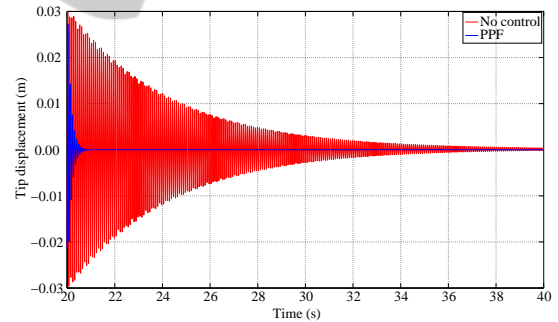

Figure 6: Tip displacement vs. time with and without control.

In the FFT spectrum diagram which is shown in Figure 7, the effect of the *PPF* controller on the amplitude of the peak displacement of the smart beam and its magnitude is illustrated.

4.2 Strain Rate Feedback Control (*SRF*)

The *SRF* control is used for active damping of a flexible space structure as in (Fei and Fang, 2006). With this technique, the structural velocity coordinate is fed back to the compensator while the compensator position coordinate multiplied by a negative gain is fed
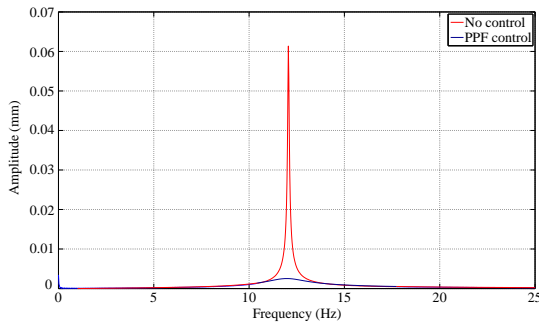
Figure 7: The FFT spectrum of the smart beam.

Figure 8: Tip displacement vs. time with and without control.

Figure 9: The FFT spectrum of the smart beam.

back to the structure. *SRF* has a wider active damping region and it can stabilize more than one mode if given a sufficient bandwidth.

The *SRF* model is presented as

$$\ddot{\xi} + 2\zeta\dot{\xi} + \omega^2\xi = -G\omega^2\eta \quad (16)$$

$$\ddot{\eta} + 2\zeta_c\omega_c\dot{\eta} + \omega_c\eta = \omega c^2\dot{\xi} \quad (17)$$

Similar to what has been done during the design of the *PPF* controller, it's also supposed that

$$\zeta = \zeta_c \quad (18)$$

$$\omega_c = \omega \quad (19)$$

To validate this supposition, the structure motion at the steady state for a single *DOF* system can have the form

$$\xi(t) = \alpha e^{i\omega t} \quad (20)$$

and the output of compesator at steady state will be

$$\eta = \beta e^{i(\omega + \frac{\pi}{2} - \phi)} \quad (21)$$

where

$$\phi = \tan^{-1}\left(\frac{2\zeta_c(\frac{\omega}{\omega_c})}{(1 - \frac{\omega^2}{\omega_c^2})}\right) \quad (22)$$

And magnitude β is given by

$$\beta = \frac{\alpha}{\sqrt{(1 - \frac{\omega^2}{\omega_c^2})^2 + (2\zeta_c\frac{\omega}{\omega_c})^2}} \quad (23)$$

When $\omega = \omega_c \Rightarrow \frac{\omega}{\omega_c} = 1$, then $\varphi = \frac{\pi}{2}$

$$\Rightarrow \ddot{\xi} + 2\zeta\omega\dot{\xi} + (\omega^2 + G\beta\omega^2)\xi = 0 \quad (24)$$

In this case, there will be an increase in the stiffness of the structure (active stiffness). Moreover, the stability condition is not clearly defined due to the fact that the closed-loop damping and stiffness matrices of the whole system cannot be symmetrized (Newman, 1992). The *SRF* controller has shown to be very effective in damping the first eigenmode of the smart beam. This is shwon in (Figure 8) and (Figure 9).
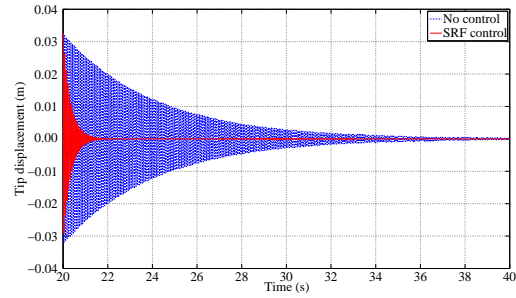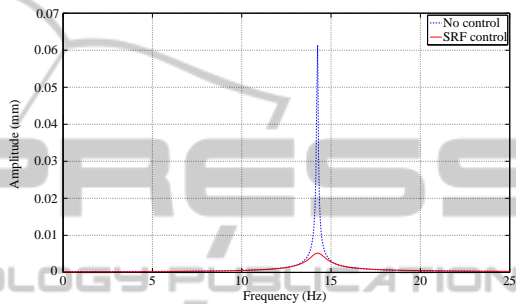
4.3 Comparison of Results of Controllers

Comparing the results of the *PPF* and *SRF* controllers, together with the Lyapunov stability control strategy from (Ghareeb and Schmidt, 2012), some important facts were noticed. Firstly, the *SE* technique has proved its efficiency by demanding low effort and small computation time. Secondly, it was concluded that the *PPF* controller needed much less time to stabilize the system, in comparison to the other controllers. This is shown in Figure 10 and Figure 11.

Thus, when the *PPF* controller was implemented, it took about 0.8 seconds to stabilize the tip displacement, while with other controllers it took about 2 seconds.

The SRF and Lyapunov control strategies produced similar results. This is due to the fact that in both controllers, the velocity was the input parameter to the system.

The effectiveness of the *PPF* is shown also in Figure 12 where the amplitude of the resonance of the first natural frequency is highly reduced in comparison to the other control strategies.
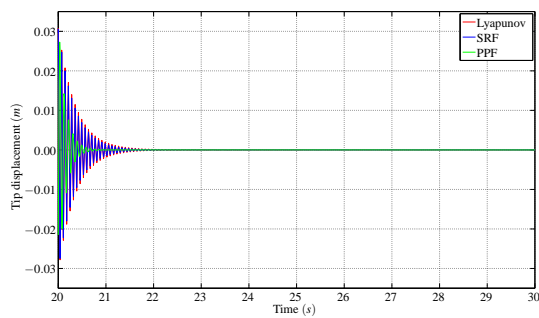
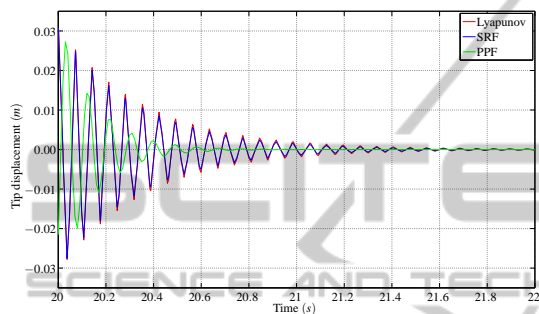Figure 10: Tip displacement vs. time (SE model).

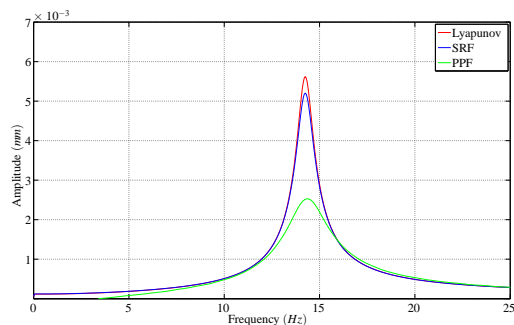Figure 11: Tip displacement vs. time in a zoomed region of Figure 10.

Figure 12: The FFT spectrum of the smart beam.

5 CONCLUSIONS

In this work, the basic procedures for the modeling and simulation of a smart beam were presented. At the beginning, the relation between actuator velocity and actuator moment was derived. A *FE* model was created and the damping coefficients were calculated. A *SE* model was then deduced from the *FE* model. Different linear controllers were designed and implemented on the *SE* to control the free body vibrations of the cantilevered beam which was excited by its first eigenmode. The controllers proved to be very effective and the results were shown and compared. In the future, other types of controllers will be designed and implemented. Nevertheless, more eigenmodes will be controlled and the possibility to implement the controllers experimentally will be checked.

REFERENCES

Adhikari, S. and Woodhouse, J. (2001). Identification of damping: Part 1, viscous damping. *Journal of Sound and Vibration*, 243, no.1:43–61.

Alipour, A. and Zareian, F. (2008). Study rayleigh damping in structures; uncertainties and treatments. In *The 14th World Conference on Earthquake Engineering*, Beijing, China.

Allik, H. and Hughes, T. (1970). Finite element method for piezoelectric vibration. *International Journal for Numerical Methods in Engineering*, 2:151–157.

Bailey, T. (1984). Distributed-parameter vibration control of a cantilever beam using a distributed-parameter actuator. Master's thesis, Massachusetts Institute of Technology.

Bailey, T. and Jr., J. H. (1985). Distributed piezoelectric-polymer active vibration control of a cantilever beam. *AIAA Journal of Guidance and Control*, 6, no.5:605–611.

Block, J. and Strganan, T. (1998). Applied active control for a nonlinear aeroelastic structure. *Journal of Guidance, Control, and Dynamics*, 21, no.6:838–845.

Craig, R. and Bampton, M. (1968). Coupling of substructures for dynamic analyses. *AIAA Journal*, 6, no.7:1313–1319.

Crawley, E. and Anderson, E. (1990). Detailed models of piezoceramic actuation of beams. *Journal of Intelligent Material Systems and Structures*, 1, no.1:4–24.

Crawley, E. F. and de Luis, J. (1987). Use of piezoelectric actuators as elements of intelligent structures. *AIAA Journal*, 25, no.10:1373–1385.

Fanson, J. and Caughey, T. (1990). Positive position feedback control for large space structures. *AIAA Journal*, 28, no.4:717–724.

Fanson, J. and Chen, J. (1986). Structural control by the use of piezoelectric active members. *Proceedings of NASA/DOD Control-Structures Interaction Conference, NASA CP-2447*, 2:809–830.

Fei, J. and Fang, Y. (2006). Active feedback vibration suppression of a flexible steel cantilever beam using smart materials. *Proceedings of the First International Conference on Innovative Computing, Information and Control (ICICIC'06)*.

Gawronski, W. (2004). *Advanced Structural Dynamics and Active Control of Structures*. Springer.

Ghareeb, N. (2013). *Design and Implementation of Linear Controllers for the Active Control of Reduced Models of Thin-Walled Structures*. PhD thesis, RWTH Aachen University of Technology.

Ghareeb, N. and Radovcic, Y. (August 2009). Fatigue analysis of a wind turbine power train. *DEWI magazin*, 35:12–16.

Ghareeb, N. and Schmidt, R. (2012). Modeling and active vibration control of a smart structure. In *Proceedings of the 9th International Conference on Informatics in Control, Automation and Robotics (ICINCO 2012)*, volume 1, pages 142–147, Rome.

Goh, C. and Caughey, T. (1985). On the stability problem caused by finite actuator dynamics in the collocated control of large space structures , 1985, vol. 41, no. 3, pp. 787-802. *International Journal of Control*, 41, no.3:787–802.

Moheimani, S. and Fleming, A. (2006). *Piezoelectric Transducers for Vibration Control and Damping*. Springer.

Newman, S. (1992). Active damping control of a flexible space structure using piezoelectric sensors and actuators. Master's thesis, U.S. Naval Postgraduate School, CA.

Piefort, V. (2001). *Finite Element Modelling of Piezoelectric Active Structures*. PhD thesis, Universit Libre de Bruxelles, Belgium.

Varadan, V., Lim, Y., and Varadan, V. (1996). Closed loop finite-element modeling of active/passive damping in structural vibration control. *Smart Materials and Structures*, 5, no.5:685–694.

Waghulde, K., Sinha, B., Patil, M., and Mishra, S. (2010). Vibration control of cantilever smart beam by using piezoelectric actuators and sensors. *International Journal of Engineering and Technology*, 2, no.4:259–262.